Human adipocytes from the subcutaneous superficial layer have greater adipogenic potential and lower *PPARG* DNA methylation levels than deep layer adipocytes

（ヒト皮下浅層由来の脂肪細胞は深層より脂肪分化能が高く、

PPARG の DNA メチル化レベルは深層より低い）

千葉大学大学院医学薬学府

先端医学薬学専攻

（主任：佐藤兼重教授）

小坂　健太朗

Abstract

Background

Human subcutaneous fat tissue consists of two layers: superficial adipose tissue (SAT) and deep adipose tissue (DAT). Some recent reports suggest that a disproportionate accumulation of DAT is related to obesity-associated metabolic complications. However, the differences in adipocyte function between SAT and DAT are unclear.

Materials and Methods

To clarify the differences in human adipocyte characteristics between SAT and DAT, human ceiling culture-derived proliferative adipocytes (ccdPAs) were primary cultured from SAT and DAT of lean females. Differences in adipogenic differentiation potential and sensitivity to exogenous adipogenic factors were examined. Epigenetic modification of the CpG island DNA methylation levels of genes related to adipogenesis was measured.

Results

In histological analyses, the mean adipocyte size in SAT was significantly larger than that in DAT (8741 ± 416 vs. 7732 ± 213 μm^2, $P < 0.05$). Primary cultured adipocytes from SAT showed significantly greater adipogenesis than did those of DAT. Sensitivity to partial adipogenic stimulation was significantly different between ccdPAs of SAT and DAT. PPAR-γ protein expression and leptin protein secretion from ccdPAs were

significantly higher in SAT than DAT. DNA methylation levels of *PPARG* were significantly lower in ccdPAs of SAT than DAT.

Conclusion

Adipocyte size was larger in SAT than DAT in vivo. This is consistent with the findings of an in vitro study that, compared with ccdPAs in DAT, ccdPAs in SAT have higher adipogenic potential and lower DNA methylation levels of *PPARG*.

Keywords:

subcutaneous tissue; adipocyte; adipogenesis; epigenetics;

Introduction

Subcutaneous tissue is divided into two layers: superficial adipose tissue (SAT) and deep adipose tissue (DAT) (7). The superficial fascia is the fibrous membrane separating the subcutaneous tissue into these two layers. The two-layer structure of human subcutaneous tissue can be recognized easily, especially in the abdomen and dorsum (Fig. 1A). SAT has thick fibrous septa and cuboid-shaped fat lobules, whereas DAT has thin fibrous septa and flat-shaped fat lobules. Based on anatomical studies, these two layers are reported to have different physical functions: SAT protects the human body from external compression, whereas DAT functions to stretch or slide the skin in response to external force (25).

Location-specific functional differences in adipocytes between visceral and subcutaneous fat have been well investigated (24). However, physiological functional differences between SAT and DAT are poorly understood. Recent studies showed that a disproportionate accumulation of DAT, but not SAT, was related to impaired systemic metabolism, which is similar to the well-known relationship between visceral fat accumulation and metabolic impairment (10, 17, 23, 28, 35). However, little is known regarding the association of cellular functional differences between the two layers of subcutaneous fat and impaired metabolism.

We hypothesized that adipocyte function differs between SAT and DAT. To test this hypothesis, we analyzed the cellular functions of human primary cultured adipocytes from SAT and DAT.

Methods

Ethics

We obtained human adipose tissue from surplus portions of abdominal flaps obtained from metabolically healthy lean Japanese female patients who underwent breast reconstructive surgery. Lean was defined as normal body weight (18.5 kg / m^2 ≤ body mass index (BMI) < 25.0 kg / m^2) according to the definition of the Japan Society for the Study of Obesity (38). The study protocol was approved by the Ethics Committee of Chiba University School of Medicine (approval number 1510). Written informed consent was obtained from the subjects. All studies were performed according to the guidelines of the Declaration of Helsinki.

Microscopic analyses of adipose tissue

Full-thickness skin samples including epidermal, dermal, and subcutaneous tissues above the muscle fascia of the obliquus externus abdominis muscle were obtained and fixed in 20% neutral buffered formalin solution (Wako, Osaka, Japan) for hematoxylin-eosin (HE), Azan, Masson-Goldner (MG) and Elastica van Gieson (EVG) staining analyses. Immunohistochemical staining of fatty acid binding protein-4 (FABP4), which is a specific marker of the adipocyte membrane, was also performed on the samples after fixation using tissue fixative G-Fix (#STF-01, Genostaff, Tokyo, Japan), which is 10% neutral buffered formalin containing picric acid. As the primary antibody, anti-

FABP4 rabbit antibody (#15872-1-AP, Proteintech, Chicago, IL, USA) was used. We counted the number of adipocytes / mm^2 on FABP4-stained images and compared these values between SAT and DAT. The mean adipocyte area was calculated under a BZ-9000 microscope (Keyence, Osaka, Japan) as follows: area of the field of view (μm^2) / number of adipocytes in the field of view.

Primary cell culture and adipogenic induction

First, we prepared human primary cultured ceiling culture-derived proliferative adipocytes (ccdPAs) and stromal vascular fraction (SVF)-derived progenitor cells (adipose-derived stem cells, ASCs) from SAT and DAT separately according to Kuroda et al.(20). Under the ethical approval described above, primary cultured ccdPAs and ASCs were harvested from subcutaneous adipose tissue of discarded area of abdominal flaps of metabolically healthy lean (18.5 kg / $m^2 \leq$ body mass index (BMI) < 25.0 kg / m^2) Japanese female (age range: 41-50). Briefly, fat tissue was weighed, and 1.0 gram tissue was digested with gentle shaking at 100 rpm for 1 hour at 37°C in 3 mL Hank's balanced salt solution (Sigma-Aldrich, St. Louis, MO, USA) containing 2 mg / mL collagenase (Wako) and 40 μg / mL gentamicin (Gentacin, Schering-Plough, Kenilworth, NJ, USA). This solution was then diluted with 10 mL Dulbecco's modified Eagle's medium/F12-HAM (DMEM/HAM) (Sigma-Aldrich) supplemented with 20% fetal bovine serum (FBS) (SAFC Biosciences, Lenexa, KS, USA) and 40 μg / mL

gentamicin, mixed, and centrifuged at 400 × g for 1 minute. The dilution steps were repeated four times to collect the floating cell fraction. The floating fraction was filtered through a 500-μm mesh (Netwell, Corning , NY, USA) and seeded into flasks filled with DMEM/HAM supplemented with 20% FBS and 40 μg / mL gentamicin and then incubated at 37°C, 5% CO_2 for 7 days. After 7 days of ceiling culture, cells that grew on the ceiling surfaces were collected as ccdPAs and seeded into flasks for the subsequent steps. The sediment from each centrifugation step was collected and cultured as ASCs in DMEM/HAM with 20% FBS and 40 μg / mL gentamicin at 37°C, 5% CO_2 for 7 days. To compare adipocytes between SAT and DAT, four populations of cells were cultured: ccdPAs obtained from SAT (CS), ccdPAs obtained from DAT (CD), ASCs obtained from SAT (AS) and ASCs obtained from DAT (AD). Each cell type harvested was cultured and passaged once a week in DMEM/HAM (Sigma-Aldrich) containing 20% FBS (SAFC Biosciences) and 40 μg / mL gentamicin (Schering-Plough). In each experiment, we used cells cultured 30-60 days after harvest. For adipogenic induction, after confirming the confluency of seeded cells (5-7 days from seeding), we changed the medium to adipogenic differentiation medium (#PT-8002, Lonza, Basel, Switzerland) containing 10% FBS and cultured the cells for 14 days. To compare adipogenic induction among the four cell populations (CS, CD, AS, and AD), we stained the differentiated cells with Oil Red O (Wako) or BODIPY (Life

Technologies, Carlsbad, CA, USA). On BODIPY-stained images, each total droplet area (green staining) per field of view (1.6×10^6 μm^2) was calculated. These microscopic studies were performed using a BZ-9000 microscope with the GFP OP-66835 filter (excitation wavelength 480 nm, emission wavelength 515 nm; Keyence) and were analyzed by the BZ-H2C application (Keyence).

Partial adipogenic stimulation

This experiment was designed to compare the effect of partial adipogenic stimulation on primary cultured ccdPAs harvested from SAT and DAT (CS and CD, respectively). After culturing, according to the protocol described above, cells were partially stimulated for adipogenesis. Normal adipogenic differentiation medium (#PT-8002, Lonza) contains three important factors for adipogenic induction: insulin, 3-isobutyl-1-methylxanthine (IBMX), and dexamethasone. For partial adipogenic stimulation, we prepared three different media, each containing only two of these three factors (insulin, IBMX, or dexamethasone). After 14 days of culture in these media, total RNA was extracted using the RNeasy Mini kit (Qiagen, Venlo, Netherlands) and was reverse transcribed using the ReverTra Ace qPCR RT Master Mix kit (Toyobo, Osaka, Japan). Gene expression levels were compared using quantitative reverse transcription-polymerase chain reaction (RT-PCR), as described in detail below.

RT-PCR

cDNA synthesized from total RNA using the ReverTra Ace qPCR RT kit (Toyobo) was subjected to quantitative RT-PCR amplification using TaqMan Gene Expression Master Mix (Life Technologies) and the LightCycler 96 system (Roche Applied Science, Basel, Switzerland). mRNA expression levels of peroxisome proliferator-activated receptor gamma (*PPARG*), CCAAT/enhancer binding protein delta (*CEBPD*) and leptin (LEP) were quantified by real-time RT-PCR amplification using specific primers, all purchased from Life Technologies. The quantification of each gene was expressed as the relative mRNA level after normalization to 18S rRNA.

Adipogenic differentiation and adipogenic markers

Primary cultured ccdPAs harvested from SAT and DAT (CS and CD, respectively) and primary cultured ASCs harvested from SAT and DAT (AS and AD, respectively) were cultured in DMEM/HAM with 20% FBS and 40 μg / mL gentamicin. Two days after reaching confluency, the medium was changed to adipogenic differentiation medium (#PT-8002, Lonza). As a control, medium without insulin, IBMX, or dexamethasone was used. After 14 days of culture in adipogenic differentiation medium, total RNA was extracted using the RNeasy Mini kit (Qiagen), and quantitative RT-PCR was performed, as described above, to measure *PPARG* and *CEBPD* mRNA expression levels.

Western blot analysis of PPAR-γ

Cell pellets were derived from the differentiated and non-differentiated four cell populations (CS, CD, AS, and AD) after culturing as described above. The pellets were lysed in ice-cold radio-immunoprecipitation assay (RIPA) buffer containing protease inhibitor cocktail (Sigma-Aldrich) and incubated at 4°C for 30 min. After centrifuging twice, the supernatants were collected and measured for protein concentration using the BCA Protein Assay Kit (Thermo-Scientific, Waltham, MA, USA), with bovine serum albumin (BSA) as the standard. These protein extracts were mixed with sodium dodecyl sulfate (SDS) sample buffer, heated at 45°C for 15 min, then cooled on ice immediately. A 15-μg protein aliquot from each sample was separated by SDS-polyacrylamide gel electrophoresis on a 10% gel (ATTO, Tokyo, Japan) and transferred to a polyvinylidene difluoride membrane (Bio-Rad, Hercules, CA, USA). After blocking in Tris-buffered saline (TBS) with 0.05% Triton X100 containing 1% BSA (Nacalai, Kyoto, Japan) at room temperature for 30 min, the membrane was incubated at 4°C overnight with PPAR-γ antibody (#2435S, Rabbit mAb, ×300 dilution; Cell Signaling Technology, Beverly, MA, USA). Next, excess antibody was washed away using a solution of TBS and 0.05% Tween 20 (TBST), and the membrane was incubated with horseradish peroxidase (HRP)-conjugated anti-rabbit IgG antibody (#7074S, ×2,000 dilution; Cell Signaling Technology) at room temperature for 2 hours. After washing away the excess antibody again, the membrane was incubated with SuperSignal West Pico

Chemiluminescent Substrate (Thermo-Scientific) at room temperature for 5 min, and the signals were detected using X-ray film. To detect the glyceraldehyde-3-phosphate dehydrogenase (GAPDH) protein, as the loading control, the membrane was incubated with anti-GAPDH (#MCA4739, 0.05 μg / mL; Bio-Rad) and HRP-linked anti-mouse IgG antibodies (#7076S, ×2,000 dilution; Cell Signaling Technology). The relative densities of the detected protein bands were analyzed using ImageJ software (version 1.47; National Institutes of Health, Bethesda, MD, USA).

Enzyme-linked immunosorbent assay (ELISA)

ELISA was performed to evaluate leptin protein production quantitatively in the eight cell populations: differentiated and non-differentiated CS, CD, CS, and AD cells. Twenty-four hours after changing to serum-free medium, we analyzed leptin levels in the serum-free medium by Quantikine ELISA Kit (R&D Systems, Minneapolis, MN, USA), according to the manufacturer's instructions. Absorbance was read using the Spectramax 340 plate reader (Molecular Devices, Sunnyvale, CA, USA), and the data were analyzed using Softmax PRO software, version 2.04 (Molecular Devices).

DNA methylation profiling

DNA was extracted from undifferentiated CS and CD cells after 14 days incubation in DMEM/HAM containing 20% FBS and 40 μg / mL gentamicin using the DNeasy kit (Qiagen) in accordance with the manufacturer's instructions. Genome-wide methylation

levels were measured by the HumanMethylation450 BeadChip array (Illumina, San Diego, CA, USA) according to standard protocol. Genomic DNA samples (0.5 μg) were subjected to bisulfite conversion using the EZ DNA methylation kit (Zymo-Research, Irvine, CA, USA). After alkaline denaturation, the samples were subjected to whole-genome amplification, and the resulting genomic DNA was fragmented and resuspended in hybridization buffer. After heat-denaturation, the samples were applied to the HumanMethylation450 BeadChip and hybridized for 20 hours. Primer extension and fluorochrome staining were performed. We obtained images by iScan (Illumina) and analyzed the data using GenomeStudio Methylation Module software (Illumina). The methylation ratios for individual CpG sites in each sample were represented as β-values, ranging from 0 (unmethylated) to 1 (completely methylated). We compared mean CpG island β-values among the following genes from the UCSC Genome Browser: *PPARG*, *CEBPD*, and *LEP*. CpG sites other than CpG islands, shore, shelf and open sea regions, were not considered in this analysis.

Statistical analysis

Results are presented as means ± standard deviation. Statistical comparisons between groups (CS vs. CD and AS vs. AD) were made by Student's t-test. In all cases, P values < 0.05 were considered to be statistically significant. Analyses were conducted using SPSS software (version 13.0J; SPSS, Chicago, IL, USA).

Results

Adipocytes of SAT are larger than those of DAT in lean subjects

Low-power microscopic examination of a HE-stained section demonstrated the two layers of the lower lateral region of human abdominal subcutaneous adipose tissue, i.e., SAT and DAT (Fig. 1B). The thickness of SAT was larger than that of DAT. The superficial fascia, which separates subcutaneous tissue into SAT and DAT, is a multi-layered structure consisting mostly of collagenous fiber and nuclei, according to Azan, MG, and EVG staining analyses (Fig. 1C). It was difficult to identify other components, such as elastic or muscle fibers, in the superficial fascia.

The numbers of adipocytes per unit area in SAT and DAT were counted on images stained with FABP4, a specific marker of the adipocyte membrane (Fig. 1D). The mean number of adipocytes per unit area was significantly lower in SAT than DAT (1134 ± 68 vs. 1280 ± 44 / mm^2, $P < 0.05$). The mean adipocyte size was significantly larger in SAT than in DAT (8741 ± 416 vs. 7732 ± 213 μm^2, $P < 0.05$).

These results indicate an obvious two-layered structure in the lateral abdominal subcutaneous tissue in humans and significant differences in adipocyte size between SAT and DAT. There were differences found between SAT and DAT not only in gross anatomical structures but also at the cellular level. The larger adipocyte size in SAT suggests a difference in adipogenic differentiation potential between the two layers.

Primary cultured ccdPAs of SAT have higher adipogenic potential than those of DAT

After 7 days of ceiling culture, ccdPAs showed similar morphological characteristics to those of ASCs: a fibroblast-like shape with no lipid droplets. We previously reported that ccdPAs are quite different from ASCs in cellular characteristics despite similar morphological aspects (2). One of the main differences between ccdPAs and ASCs is that the former have higher adipogenic potential even after 6 weeks of culture. We investigated the difference in adipogenic potential of ccdPAs between SAT and DAT (CS and CD, respectively). According to both oil red O and BODIPY staining, significantly higher adipogenic potential was observed in ccdPAs of SAT than those of DAT (Fig. 2). Adipogenesis in ASCs of SAT also was significantly greater than in DAT of ASCs. These results indicate that primary cultured ccdPAs of SAT maintain higher adipogenic potential than do those of DAT.

Sensitivity to partial adipogenic stimulation differs between ccdPAs of SAT and DAT

We previously reported significant differences between ccdPAs and ASCs in their sensitivity to partial adipogenic stimulation, reflecting differences in cellular function (2). Here, we examined differences between SAT and DAT in ccdPAs sensitivity to adipogenic differentiation factors and observed significant differences between the two tissue layers (Fig. 3). In the absence of insulin, there was no significant difference in mRNA expression of *PPARG* between ccdPAs of SAT and DAT. In contrast, *CEBPD*

mRNA expression was significantly lower in ccdPAs of SAT than those of DAT, whereas leptin mRNA expression was significantly higher in SAT ccdPAs. In the absence of IBMX, *PPARG* and *LEP* mRNA expression levels were significantly higher in ccdPAs of SAT compared with DAT; in contrast, *CEBPD* mRNA expression was significantly lower in SAT versus DAT ccdPAs. In the absence of dexamethasone, *PPARG* expression was significantly higher in ccdPAs of SAT than those of DAT, and the *LEP* mRNA expression level was below the detection limit in ccdPAs of both SAT and DAT.

These results indicate significant differences in cellular sensitivity to adipogenic induction factors between ccdPAs of SAT and DAT.

PPAR-γ expression is higher in ccdPAs of SAT versus DAT

PPAR-γ is a master regulator of adipogenic differentiation. Adipogenic differentiation medium significantly increased *PPARG* expression in both ccdPAs and ASCs (Fig. 4A). *PPARG* mRNA expression in ccdPAs of SAT was significantly higher than in those of DAT. The PPAR-γ protein level of ccdPAs was also significantly higher in SAT than in DAT (Fig. 4B). In contrast, mRNA expression of *CEPBD*, which is involved in adipogenic differentiation, was significantly lower in SAT versus DAT ccdPAs (Fig. 4C). Leptin secretion was significantly higher from ccdPAs of SAT than those of DAT when grown in adipogenic differentiation medium (Fig. 4D).

These results indicate that primary cultured human adipocytes of SAT have higher PPAR-γ expression potential than those of DAT in response to adipogenic induction.

PPARG DNA methylation levels are lower in ccdPAs of SAT versus DAT

Recent studies suggest that epigenetic modification plays an essential role in defining cellular differentiation (1, 11). Higher methylation levels in promoter regions, which are a form of epigenetic modification, are associated with downregulation of gene expression. In most of the CpG islands evaluated within *PPARG* (9 of 11), the mean DNA methylation levels were lower in ccdPAs of SAT than those of DAT. The differences were statistically significant for two of these CpG islands, cg04748988 and cg18887186. In contrast, 2 of 9 CpG islands of *CEBPD*, cg18923221 and cg22280940, the mean DNA methylation levels were significantly higher in ccdPAs of SAT versus DAT. There were no statistically significant differences in the DNA methylation levels of *LEP* CpG islands between ccdPAs of SAT versus DAT.

These results indicate significant differences in epigenetic modification of the adipogenic genes, *PPARG* and *CEBPD*, between SAT and DAT ccdPAs, consistent with the mRNA and protein expression results.

Discussion

In this study, we confirmed a difference in adipocyte function between the SAT and DAT layers of subcutaneous tissue in lean female subjects. Primary cultured human adipocytes from SAT showed significantly higher adipogenic potential compared with those of DAT. We also showed lower DNA methylation levels of *PPARG* in SAT versus DAT adipocytes, suggesting that PPAR-γ is more likely to be expressed in adipocytes of SAT compared with DAT.

The two layers of subcutaneous tissue in mammals, SAT and DAT, which are separated by the superficial fascia, are easily distinguishable with various imaging modalities (9, 10, 13, 25). Our histological study also showed the obvious structural findings that subcutaneous adipose tissue is divided by multi-layered superficial fascia consisting of collagen fiber and nuclei. Regarding the physical properties, Nakajima et al. reported that SAT is the protective adipofascial system and DAT the lubricant adipofascial system (25). However, little is known about the cellular functional differences between SAT and DAT. Our study is the first to verify differences in cellular function between SAT and DAT using primary cultured human adipocytes.

Our histological study of subcutaneous tissue from lean subjects showed greater SAT than DAT thickness. In plastic surgery, from various skin surgical experiences in lean subjects, subcutaneous tissue has been found to consist mainly of SAT rather than DAT.

On the contrary, liposuction in obese subjects is performed on DAT rather than SAT because of the greater abundance of DAT (8, 21). This is supported by 3-Tesla magnetic resonance imaging studies that showed a steady increase in the proportion of DAT and a decrease in the proportion of SAT with increasing obesity (28). Our results suggest that in normal metabolic lean subjects, SAT adipocytes are more likely to be mature compared with DAT adipocytes.

Our histological study on the subcutaneous adipose tissue of lean subjects showed that the mean adipocyte size in SAT was larger than that in DAT. This is consistent with other reports (4, 5, 23, 34). Marinou et al. reported smaller adipocyte sizes in DAT of lean subjects, but equal adipocyte sizes between SAT and DAT of obese subjects (23). Wan et al. reported that the difference in size of adipocytes between SAT and DAT exists not only in the trunk but also in the face (37). However, it is unclear why adipocytes are larger in SAT than DAT. Our results provided a link between adipogenic potential in vitro and adipocyte size in vivo. Our finding that adipocytes of SAT have higher adipogenic potential than those of DAT due to lower DNA methylation levels of the *PPARG* promoter may be one explanation for the adipocyte size difference between SAT and DAT in vivo.

Differences in adipocyte function are also shown by the differences in mRNA expression patterns induced by partial adipogenic stimulation. In our previous report

regarding differences between ccdPAs and ASCs, the mRNA expression patterns induced by the various adipogenic factors suggest differences in cell function (2). Similarly, adipocytes of SAT and DAT showed quite different mRNA expression patterns induced by variations in culture medium, indicating the existence of substantial cellular functional differences between adipocytes of SAT and DAT, suggesting differences in receptor status, cell signaling, and transcriptional control.

Our study showed that primary cultured adipocytes of SAT have higher PPAR-γ protein expression and higher leptin secretion levels than those of DAT. Recent studies have indicated a relationship between disproportionate accumulation of DAT and impaired systemic metabolism, similar to the well-known relationship between visceral fat accumulation and metabolic impairment(10, 17, 23, 28, 35). As an example, we previously reported that adipocytes of visceral fat, but not subcutaneous fat, secrete TNF-α and exacerbate insulin sensitivity (30). Several reports showed that DAT accumulates disproportionally more than does SAT in obese subjects, and the proportion of DAT in subcutaneous adipose tissue is a predictor of obesity-associated disorders (10, 23, 36). Walker et al. reported that adiponectin protein expression is higher in SAT than DAT in lean individuals, similar to our results that primary cultured adipocytes of SAT express more *PPARG* and *LEP* than do those of DAT (36). Cancello et al. reported that in obese individuals, tissue mRNA expression levels of *PPARG* and

adiponectin in subcutaneous adipose tissue were significantly lower in DAT, whereas those of HIF-1α and TNF-α were significantly higher (5).

Analysis of the differences in adipocyte function between SAT and DAT is also import for adipocyte transplantation. We previously reported that PPAR-γ expression stimulated by bFGF is important for engraftment and maturation of transplanted adipocytes in mice (19). Transplantation of adipocytes was originally used as a method of tissue augmentation. Currently, the application of adipocyte transplantation has broadened. Adipocyte transplantation has recently been used to facilitate the wound healing process, to ameliorate scar tissue quality, and as a vehicle for gene therapy, a subject of focus for us (6, 16, 20) . We have published several previous reports on a gene therapy model using transfected adipocytes as a vehicle (14, 15, 18). In such models, the risk of malignancy-associated mutation of the transfected cells is a major problem. Shimizu et al. reported that cells with higher adipogenic potential show less susceptibility to malignancy-associated mutations (31). Based on our results that adipocytes of SAT have higher adipogenic potential than those of DAT, the former are preferable to the latter for adipocyte transplantation. However, generally, liposuction of abdominal subcutaneous tissue is performed on DAT rather than SAT because of its abundance and looseness (8). Further investigation is required to conclude whether SAT versus DAT is preferable as a donor site for adipocyte transplantation.

Epigenetic control of gene expression is a key regulator of cellular differentiation (11). In our study, the DNA methylation level of the promotor of the adipogenic master regulator gene *PPARG* was lower in adipocytes of SAT than those of DAT. Our result is consistent with a previous animal study showing that adipose tissue development is regulated by epigenetic DNA methylation of *PPARG* (32). In contrast, in our study, adipocytes of SAT showed significantly higher DNA methylation levels of *CEBPD*, another gene related to adipogenesis, than did those of DAT. CEBP-δ, in coordination with CEBP-β, induces PPAR-γ expression (12, 26). However, animal experiments have shown that PPAR-γ is indispensable for adipogenesis, whereas CEPB-δ is not necessarily indispensable, in that mice lacking *CEBPD* can exhibit adipogenesis and normal PPAR-γ expression (3, 27, 33). The DNA methylation level of *LEP* was not different between SAT and DAT adipocytes, although leptin secretion was significantly higher in the former. We believe that the higher leptin secretion from SAT adipocytes is a result of their more advanced maturation due to higher PPAR-γ expression. Further investigation is required to clarify why and when differences arise in DNA methylation levels of adipocytes between SAT and DAT.

Several reports have shown that the degree of fat accumulation is higher in DAT than SAT in obesity. However, it is controversial whether the surrounding environment of adipocytes or the intrinsic nature of adipocytes is the cause of differences in fat

accumulation (17). Our results support differences in the intrinsic nature of adipocytes between SAT and DAT. However, Boulet et al. reported that although SAT showed higher *LEP* mRNA expression levels, the cause is not intrinsic adipocyte properties but rather T lymphocyte accumulation (4). In contrast, Shultz et al. showed that differences in adipocyte function, based on epigenetic modifications, form as early as the fetal stage (29). Li et al. also showed, in a porcine study, intrinsic functional differences between the two tissue layers due to significant differences in DNA methylation levels of genes involved in cytokine production (22). Our research using primary cultured adipocytes from humans also supports the existence of intrinsic adipocyte functional differences between SAT and DAT.

In summary, we showed that human adipocytes of SAT are larger than those of DAT in vivo, and that primary cultured adipocytes harvested from SAT have higher adipogenic potential than those harvested from DAT. This is consistent with our results that DNA methylation levels of *PPARG* were lower in primary cultured adipocytes of SAT versus DAT. Our results provide a theoretical basis for physiological differences between SAT and DAT.

References

1. **Alvarez-Errico D, Vento-Tormo R, Sieweke M, and Ballestar E**. Epigenetic control of myeloid cell differentiation, identity and function. *Nat Rev Immunol* 15: 7-17, 2015.

2. **Asada S, Kuroda M, Aoyagi Y, Fukaya Y, Tanaka S, Konno S, Tanio M, Aso M, Satoh K, Okamoto Y, Nakayama T, Saito Y, and Bujo H**. Ceiling culture-derived proliferative adipocytes retain high adipogenic potential suitable for use as a vehicle for gene transduction therapy. *Am J Physiol Cell Physiol* 2011.

3. **Barak Y, Nelson MC, Ong ES, Jones YZ, Ruiz-Lozano P, Chien KR, Koder A, and Evans RM**. PPAR gamma is required for placental, cardiac, and adipose tissue development. *Mol Cell* 4: 585-595, 1999.

4. **Boulet N, Esteve D, Bouloumie A, and Galitzky J**. Cellular heterogeneity in superficial and deep subcutaneous adipose tissues in overweight patients. *J Physiol Biochem* 69: 575-583, 2013.

5. **Cancello R, Zulian A, Gentilini D, Maestrini S, Della Barba A, Invitti C, Cora D, Caselle M, Liuzzi A, and Di Blasio AM**. Molecular and morphologic characterization of superficial- and deep-subcutaneous adipose tissue subdivisions in human obesity. *Obesity (Silver Spring)* 21: 2562-2570, 2013.

6. **Caviggioli F, Maione L, Forcellini D, Klinger F, and Klinger M**. Autologous fat graft in postmastectomy pain syndrome. *Plast Reconstr Surg* 128: 349-352, 2011.

7. **Congdon ED, Edson J, and Yanitelli S**. Gross structure of the subcutaneous layer of the anterior and lateral trunk in the male. *Am J Anat* 79: 399-429, 1946.

8. **Gasperoni C, and Salgarello M**. Rationale of subdermal superficial liposuction related to the anatomy of subcutaneous fat and the superficial fascial system. *Aesthetic Plast Surg* 19: 13-20, 1995.

9. **Gensanne D, Josse G, Theunis J, Lagarde JM, and Vincensini D**. Quantitative magnetic resonance imaging of subcutaneous adipose tissue. *Skin Res Technol* 15: 45-50, 2009.

10. **Golan R, Shelef I, Rudich A, Gepner Y, Shemesh E, Chassidim Y, Harman-Boehm I, Henkin Y, Schwarzfuchs D, Ben Avraham S, Witkow S, Liberty IF, Tangi-Rosental O, Sarusi B, Stampfer MJ, and Shai I**. Abdominal superficial subcutaneous fat: a putative distinct protective fat subdepot in type 2 diabetes. *Diabetes Care* 35: 640-647, 2012.

11. **Goldberg AD, Allis CD, and Bernstein E**. Epigenetics: a landscape takes shape. *Cell* 128: 635-638, 2007.

12. **Gregoire FM, Smas CM, and Sul HS**. Understanding adipocyte differentiation. *Physiol Rev* 78: 783-809, 1998.

13. **Herlin C, Chica-Rosa A, Subsol G, Gilles B, Macri F, Beregi JP, and Captier G**. Three-dimensional study of the skin/subcutaneous complex using in vivo whole body 3T MRI: review of the literature and confirmation of a generic pattern of organization. *Surg Radiol Anat* 2015.

14. **Ito M, Bujo H, Takahashi K, Arai T, Tanaka I, and Saito Y**. Implantation of primary cultured adipocytes that secrete insulin modifies blood glucose levels in diabetic mice. *Diabetologia* 48: 1614-1620, 2005.

15. **Kitagawa Y, Bujo H, Takahashi K, Shibasaki M, Ishikawa K, Yagui K, Hashimoto N, Noda K, Nakamura T, Yano S, and Saito Y**. Impaired glucose tolerance is accompanied by decreased insulin sensitivity in tissues of mice implanted with cells that overexpress resistin. *Diabetologia* 47: 1847-1853, 2004.

16. **Klinger M, Caviggioli F, Vinci V, Salval A, and Villani F**. Treatment of chronic posttraumatic ulcers using autologous fat graft. *Plast Reconstr Surg* 126: 154e-155e, 2010.

17. **Koska J, Stefan N, Votruba SB, Smith SR, Krakoff J, and Bunt JC**. Distribution of subcutaneous fat predicts insulin action in obesity in sex-specific manner. *Obesity (Silver Spring)* 16: 2003-2009, 2008.

18. **Kubota Y, Unoki H, Bujo H, Rikihisa N, Udagawa A, Yoshimoto S, Ichinose M, and Saito Y**. Low-dose GH supplementation reduces the TLR2 and TNF-alpha expressions in visceral fat. *Biochem Biophys Res Commun* 368: 81-87, 2008.

19. **Kuramochi D, Unoki H, Bujo H, Kubota Y, Jiang M, Rikihisa N, Udagawa A, Yoshimoto S, Ichinose M, and Saito Y**. Matrix metalloproteinase 2 improves the transplanted adipocyte survival in mice. *Eur J Clin Invest* 38: 752-759, 2008.

20. **Kuroda M, Aoyagi Y, Asada S, Bujo H, Tanaka S, Konno S, Tanio M, Ishii I, K. M, Matsumoto F, Sato K, Aso M, and Saito Y**. Ceiling culture-derived

proliferative adipocytes are possible delivery vehicle for enzyme replacement therapy in lecithin:cholesterol acyltransferase deficiecy. *OpenGeneTherJ* 4: 2011.

21. **Lancerotto L, Stecco C, Macchi V, Porzionato A, Stecco A, and De Caro R**. Layers of the abdominal wall: anatomical investigation of subcutaneous tissue and superficial fascia. *Surg Radiol Anat* 33: 835-842, 2011.

22. **Li M, Wang T, Wu H, Zhang J, Zhou C, Jiang A, Li R, and Li X**. Genome-Wide DNA Methylation Changes between the Superficial and Deep Backfat Tissues of the Pig. *Int J Mol Sci* 13: 7098-7108, 2012.

23. **Marinou K, Hodson L, Vasan SK, Fielding BA, Banerjee R, Brismar K, Koutsilieris M, Clark A, Neville MJ, and Karpe F**. Structural and functional properties of deep abdominal subcutaneous adipose tissue explain its association with insulin resistance and cardiovascular risk in men. *Diabetes Care* 37: 821-829, 2014.

24. **McLaughlin T, Lamendola C, Liu A, and Abbasi F**. Preferential fat deposition in subcutaneous versus visceral depots is associated with insulin sensitivity. *J Clin Endocrinol Metab* 96: E1756-1760, 2011.

25. **Nakajima H, Imanishi N, Minabe T, Kishi K, and Aiso S**. Anatomical study of subcutaneous adipofascial tissue: a concept of the protective adipofascial system (PAFS) and lubricant adipofascial system (LAFS). *Scand J Plast Reconstr Surg Hand Surg* 38: 261-266, 2004.

26. **Rosen ED, Hsu CH, Wang X, Sakai S, Freeman MW, Gonzalez FJ, and Spiegelman BM**. C/EBPalpha induces adipogenesis through PPARgamma: a unified pathway. *Genes Dev* 16: 22-26, 2002.

27. **Rosen ED, Sarraf P, Troy AE, Bradwin G, Moore K, Milstone DS, Spiegelman BM, and Mortensen RM**. PPAR gamma is required for the differentiation of adipose tissue in vivo and in vitro. *Mol Cell* 4: 611-617, 1999.

28. **Sadananthan SA, Prakash B, Leow MK, Khoo CM, Chou H, Venkataraman K, Khoo EY, Lee YS, Gluckman PD, Tai ES, and Velan SS**. Automated segmentation of visceral and subcutaneous (deep and superficial) adipose tissues in normal and overweight men. *J Magn Reson Imaging* 41: 924-934, 2015.

29. **Schultz NS, Broholm C, Gillberg L, Mortensen B, Jorgensen SW, Schultz HS, Scheele C, Wojtaszewski JF, Pedersen BK, and Vaag A**. Impaired leptin gene expression and release in cultured preadipocytes isolated from individuals born with low birth weight. *Diabetes* 63: 111-121, 2014.

30. **Shibasaki M, Takahashi K, Itou T, Miyazawa S, Ito M, Kobayashi J, Bujo H, and Saito Y**. Alterations of insulin sensitivity by the implantation of 3T3-L1 cells in nude mice. A role for TNF-alpha? *Diabetologia* 45: 518-526, 2002.

31. **Shimizu T, Ishikawa T, Sugihara E, Kuninaka S, Miyamoto T, Mabuchi Y, Matsuzaki Y, Tsunoda T, Miya F, Morioka H, Nakayama R, Kobayashi E, Toyama Y, Kawai A, Ichikawa H, Hasegawa T, Okada S, Ito T, Ikeda Y, Suda T, and Saya H**. c-MYC overexpression with loss of Ink4a/Arf transforms bone marrow

stromal cells into osteosarcoma accompanied by loss of adipogenesis. *Oncogene* 29: 5687-5699, 2010.

32. **Sun YN, Gao Y, Qiao SP, Wang SZ, Duan K, Wang YX, Li H, and Wang N**. Epigenetic DNA methylation in the promoters of peroxisome proliferator-activated receptor gamma in chicken lines divergently selected for fatness. *J Anim Sci* 92: 48-53, 2014.

33. **Tanaka T, Yoshida N, Kishimoto T, and Akira S**. Defective adipocyte differentiation in mice lacking the C/EBPbeta and/or C/EBPdelta gene. *EMBO J* 16: 7432-7443, 1997.

34. **Tordjman J, Divoux A, Prifti E, Poitou C, Pelloux V, Hugol D, Basdevant A, Bouillot JL, Chevallier JM, Bedossa P, Guerre-Millo M, and Clement K**. Structural and inflammatory heterogeneity in subcutaneous adipose tissue: relation with liver histopathology in morbid obesity. *J Hepatol* 56: 1152-1158, 2012.

35. **Walker GE, Marzullo P, Prodam F, Bona G, and Di Blasio AM**. Obesity modifies expression profiles of metabolic markers in superficial and deep subcutaneous abdominal adipose tissue depots. *Endocrine* 46: 99-106, 2014.

36. **Walker GE, Verti B, Marzullo P, Savia G, Mencarelli M, Zurleni F, Liuzzi A, and Di Blasio AM**. Deep subcutaneous adipose tissue: a distinct abdominal adipose depot. *Obesity (Silver Spring)* 15: 1933-1943, 2007.

37. **Wan D, Amirlak B, Giessler P, Rasko Y, Rohrich RJ, Yuan C, Lysikowski J, Delgado I, and Davis K**. The differing adipocyte morphologies of deep versus

superficial midfacial fat compartments: a cadaveric study. *Plast Reconstr Surg* 133: 615e-622e, 2014.

38. **Youkou A, Hasegawa T, Suzuki K, Koya T, Sakagami T, Toyabe S, Arakawa M, Gejyo F, Narita I, and Suzuki E**. Influence of obesity on control in asthmatic Japanese patients defined by the Japanese definition of obesity. *Intern Med* 50: 1911-1916, 2011.

Fig. 1

A

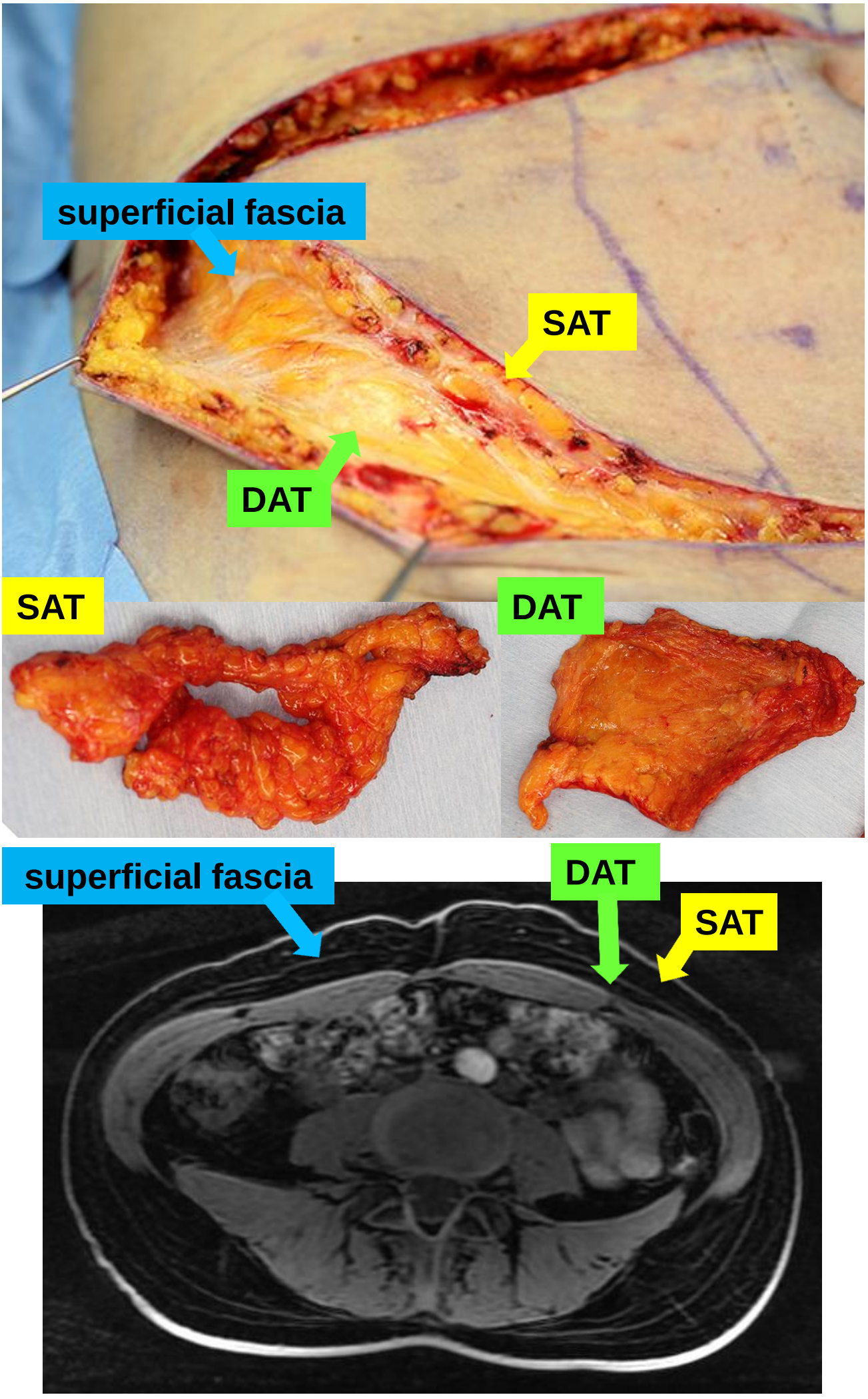
superficial fascia
SAT
DAT
SAT
DAT
superficial fascia
DAT
SAT

B

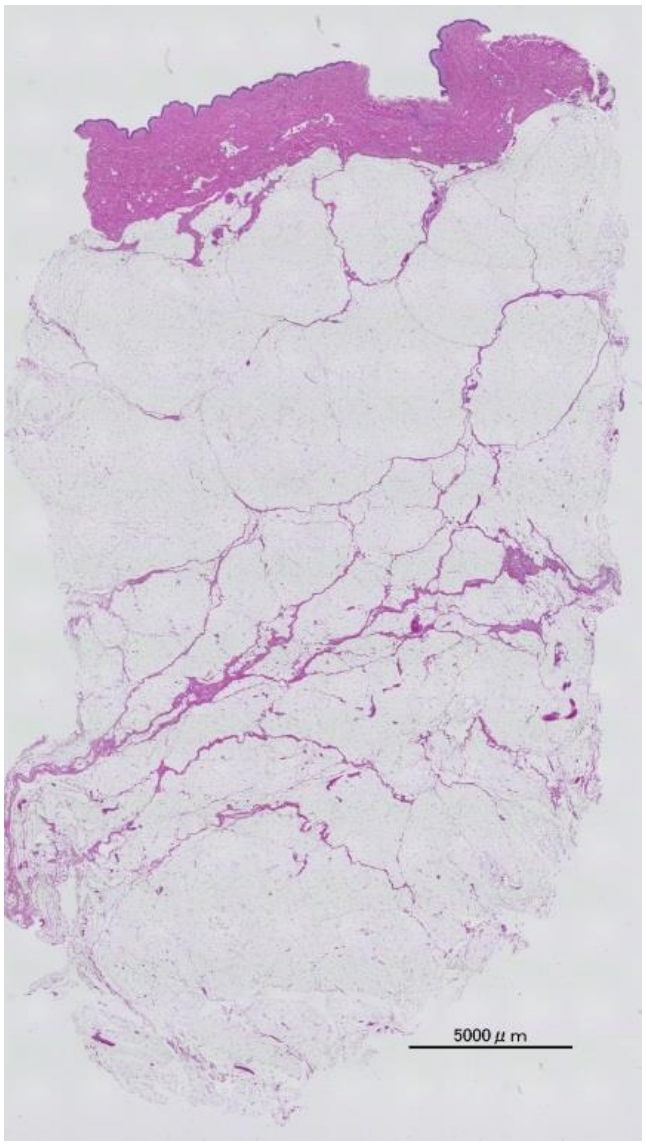

SAT

superficial fascia

DAT

C

Azan

MG

EVG

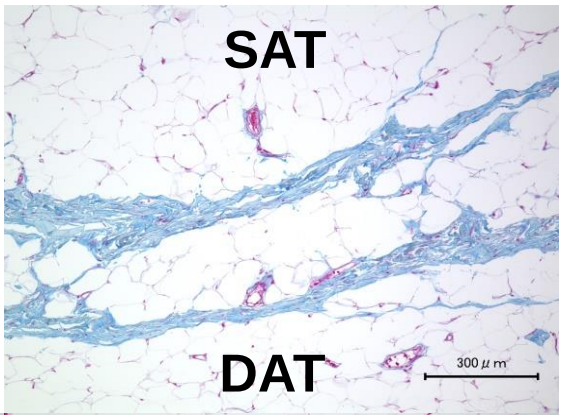

superficial fascia

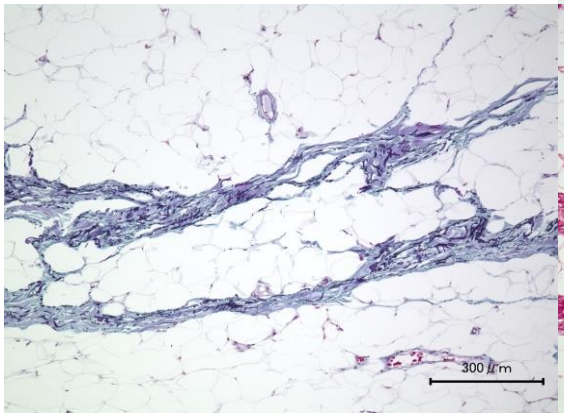

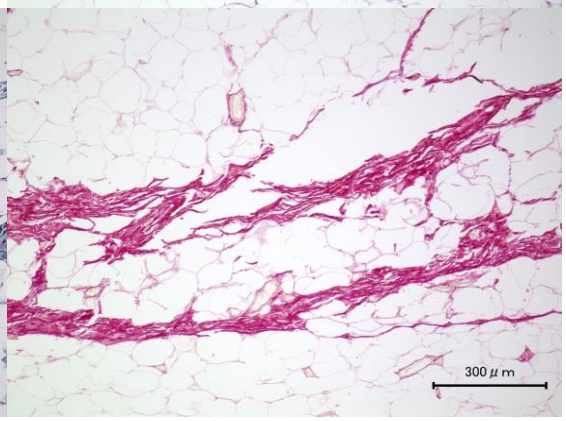

D

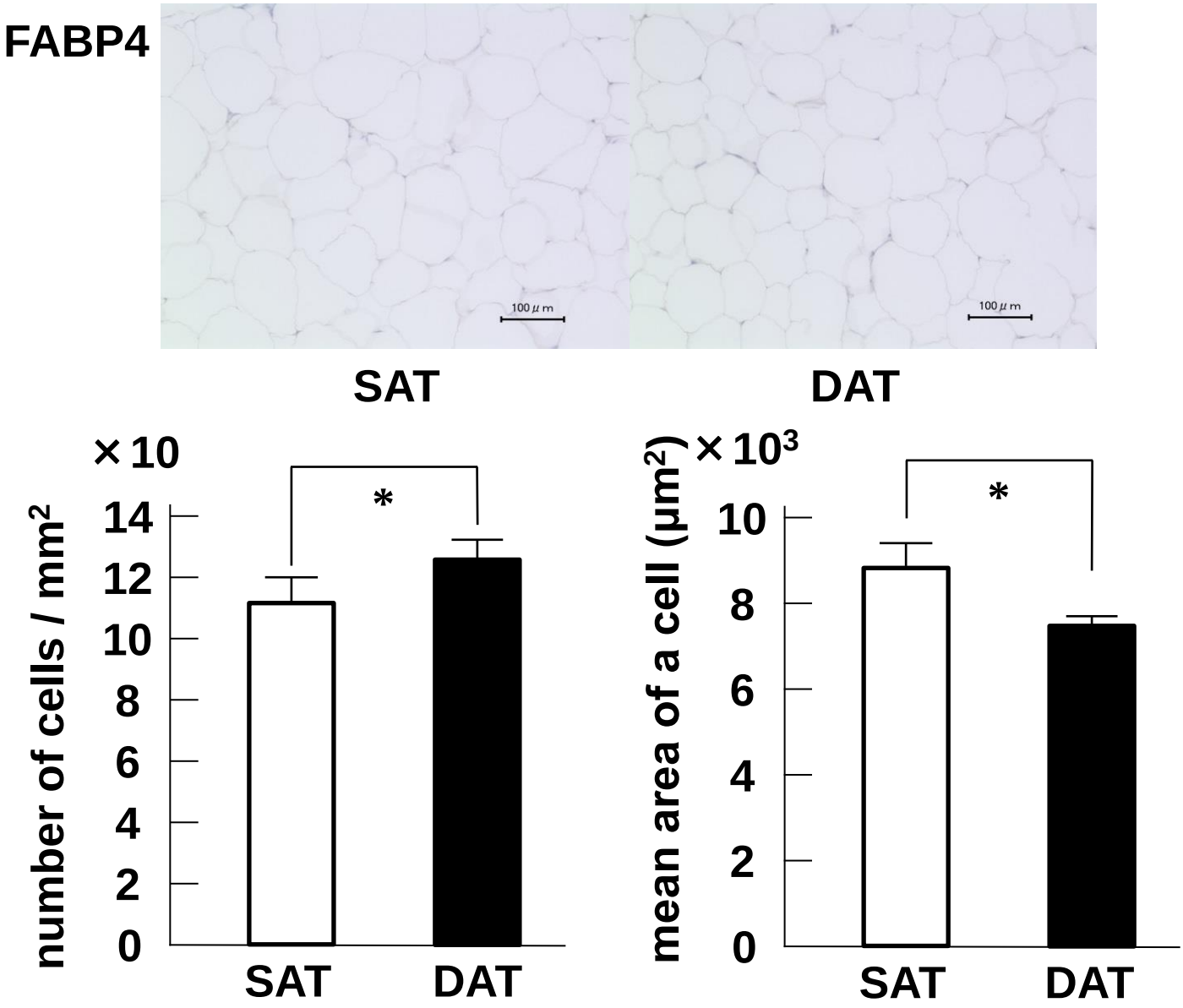
FABP4
100 μm
100 μm
SAT
DAT
× 10
number of cells / mm²
14
12
10
8
6
4
2
0
*
SAT
DAT
× 10³
mean area of a cell (μm²)
10
8
6
4
2
0
*
SAT
DAT

Fig. 2

A

Oil Red O / BODIPY

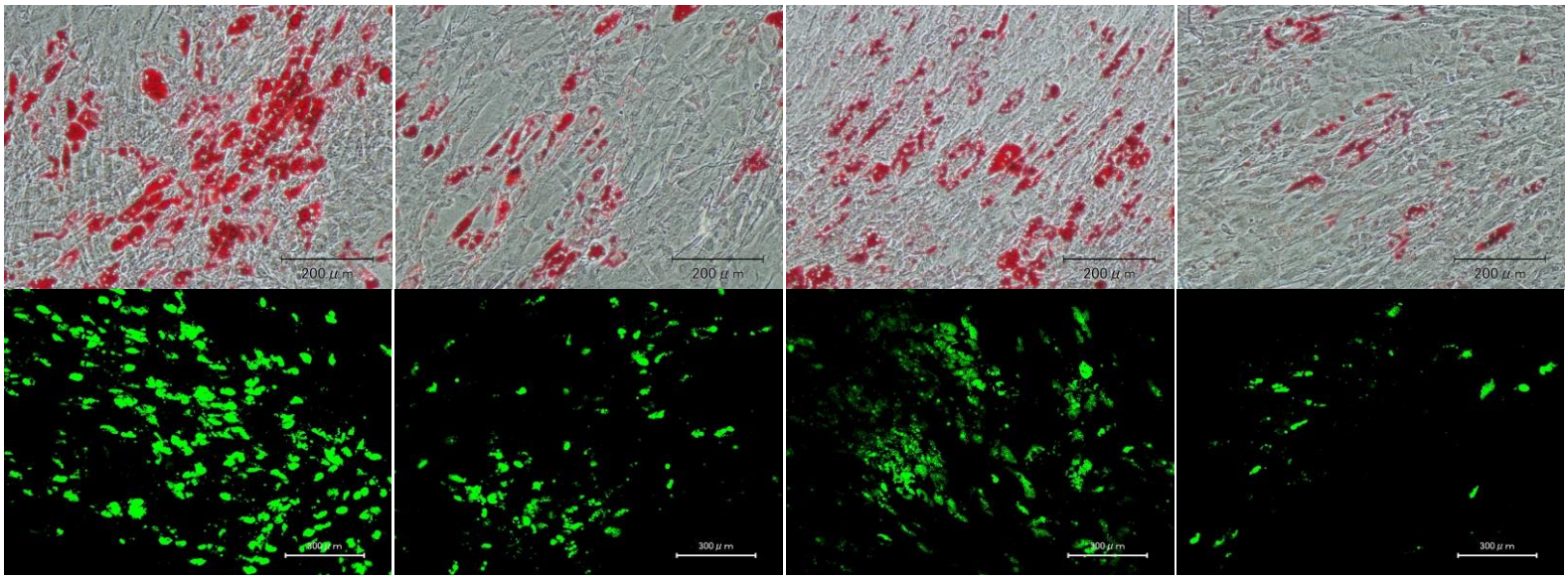

CS CD AS AD

B

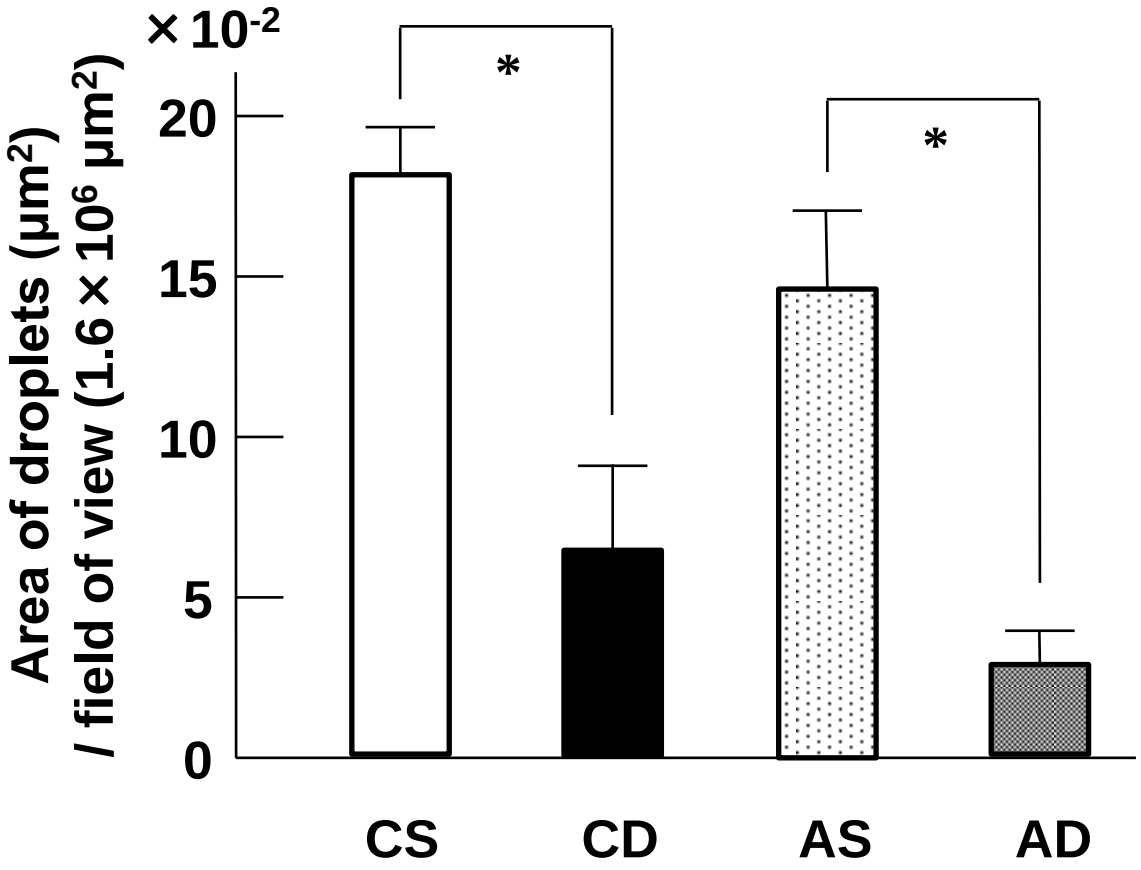

Fig. 3

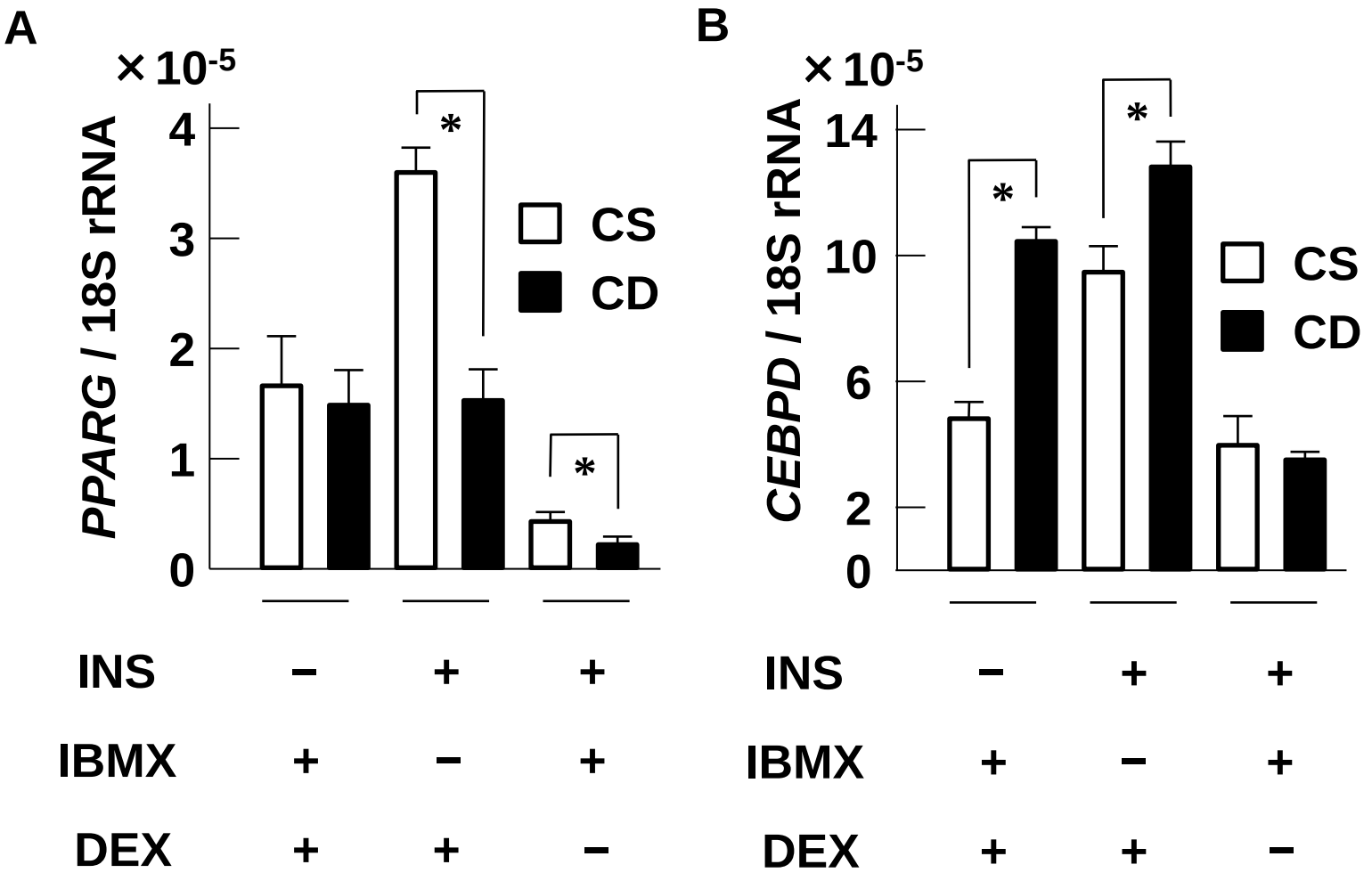
A
× 10-5
PPARG / 18S rRNA
4
3
2
1
0
*
*
CS
CD
INS − + +
IBMX + − +
DEX + + −
B
× 10-5
CEBPD / 18S rRNA
14
10
6
2
0
*
*
CS
CD
INS − + +
IBMX + − +
DEX + + −

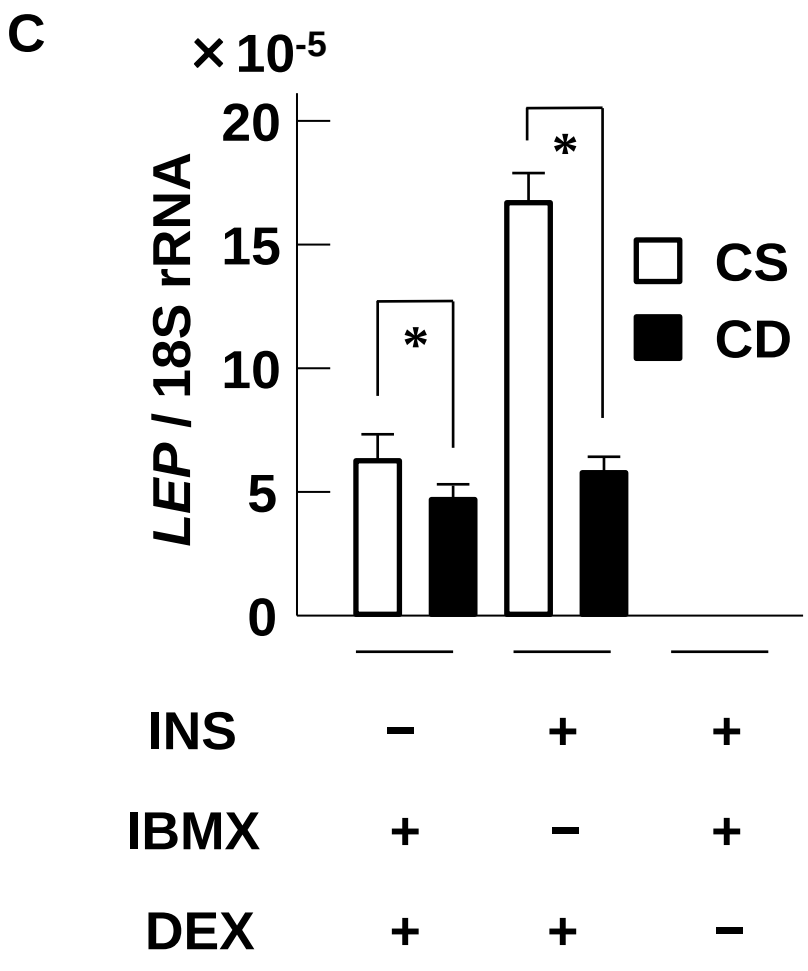
C
× 10-5
LEP / 18S rRNA
20
15
10
5
0
*
*
CS
CD
INS − + +
IBMX + − +
DEX + + −

Fig. 4

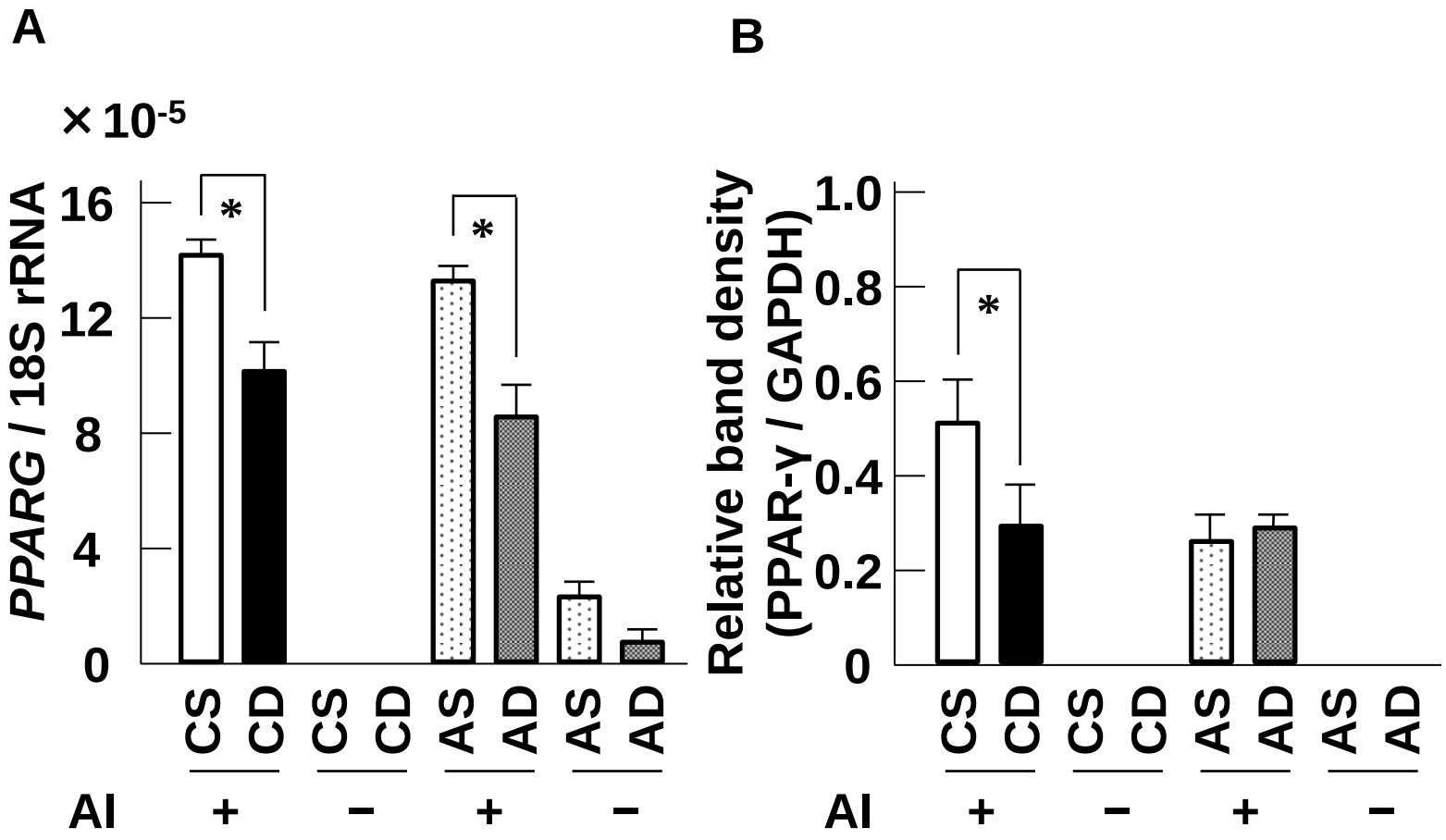
A
× 10-5
PPARG / 18S rRNA
16
12
8
4
0
*
*
CS
CD
CS
CD
AS
AD
AS
AD
Al
+
−
+
−
B
Relative band density
(PPAR-γ / GAPDH)
1.0
0.8
0.6
0.4
0.2
0
*
CS
CD
CS
CD
AS
AD
AS
AD
Al
+
−
+
−

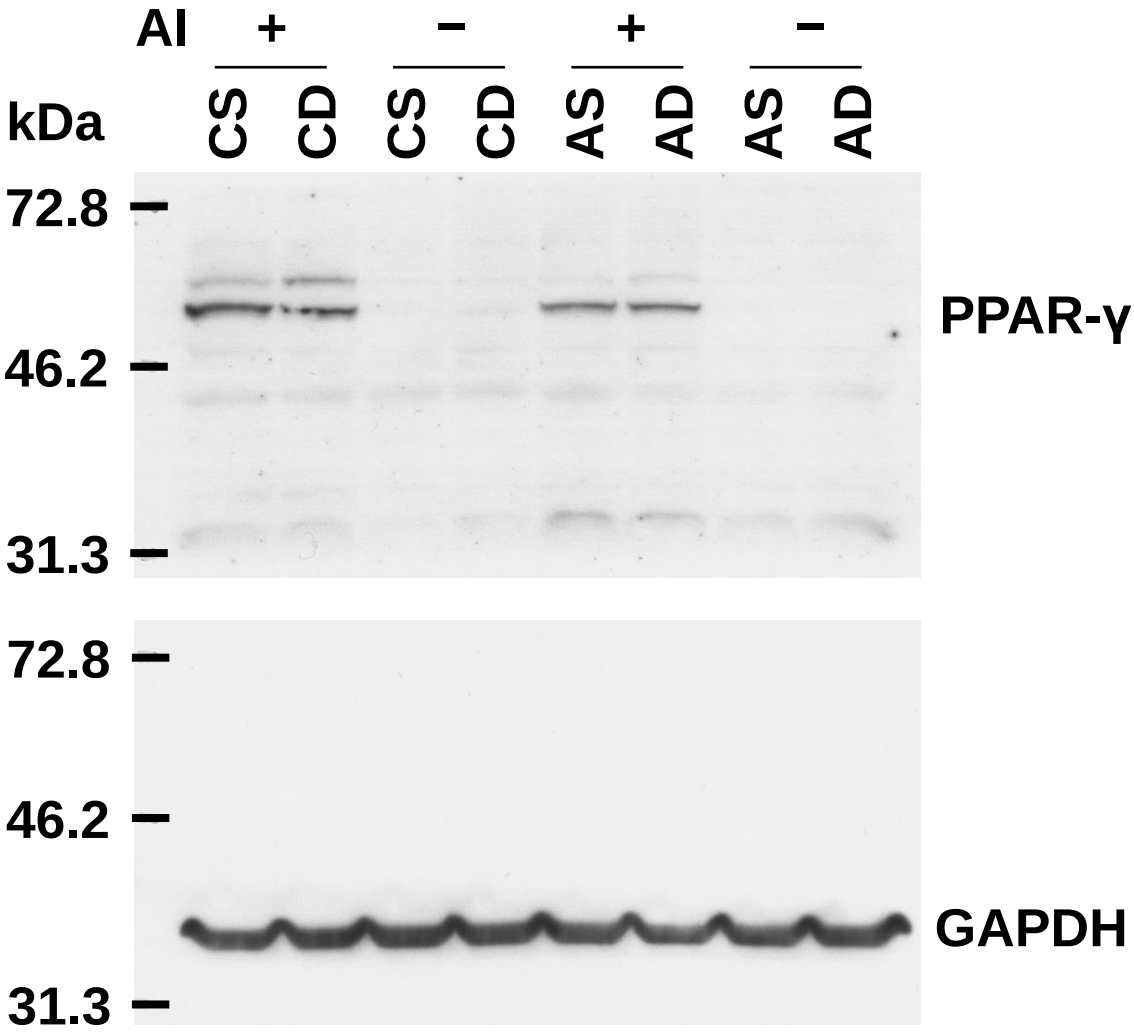
Al
+
−
+
−
kDa
CS
CD
CS
CD
AS
AD
AS
AD
72.8
46.2
31.3
PPAR-γ
72.8
46.2
31.3
GAPDH

C

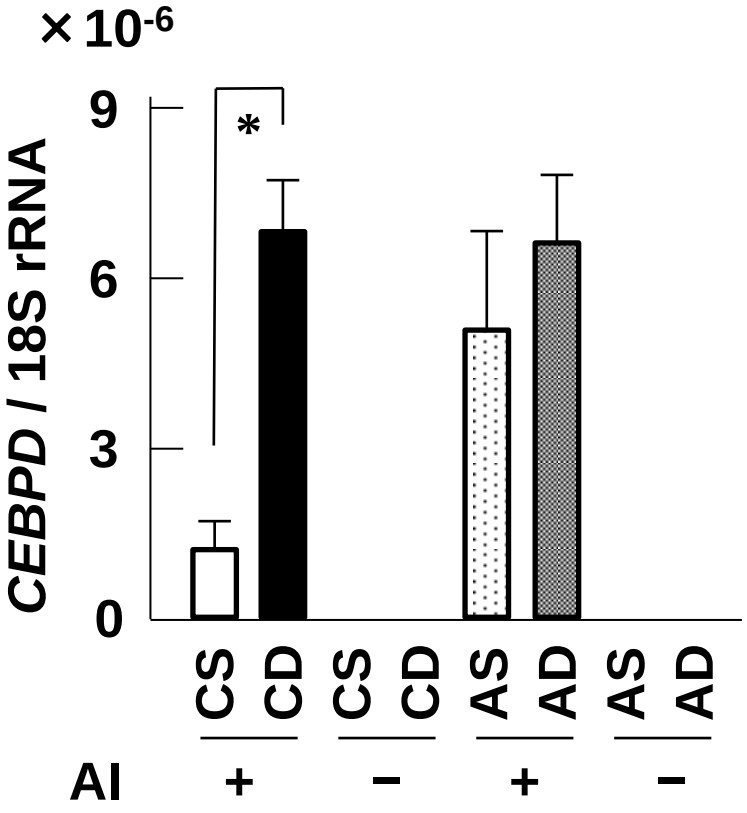
× 10-6
CEBPD / 18S rRNA
9
6
3
0
*
CS
CD
CS
CD
AS
AD
AS
AD
AI
+
−
+
−

D

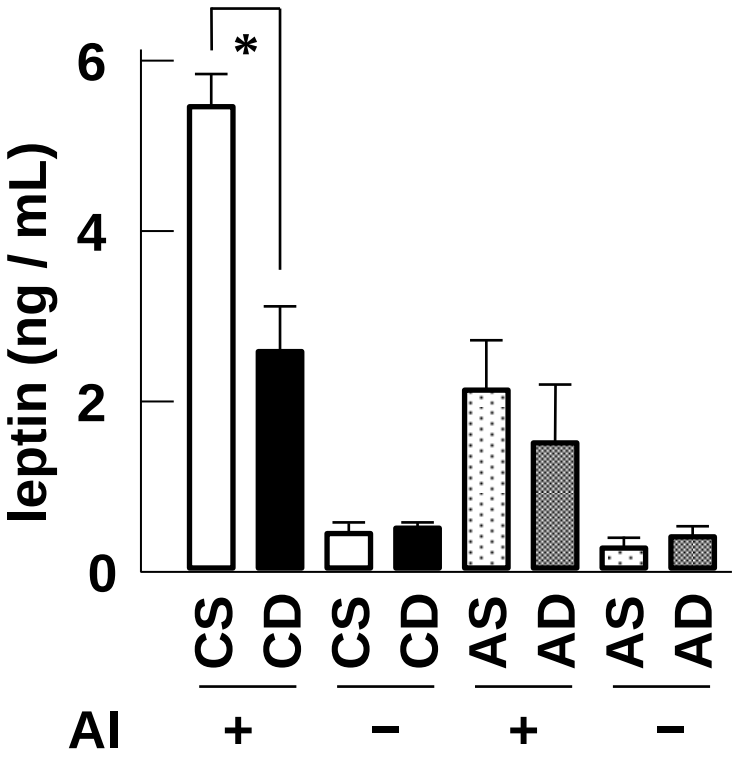
leptin (ng / mL)
6
4
2
0
*
CS
CD
CS
CD
AS
AD
AS
AD
AI
+
−
+
−

Table. 1

Gene	Probe ID	chr	Map info.	β value			
				CS ± sd	CD ± sd	p value	
PPARG	cg04632671	3	12329826	0.005 ± 0.003	0.004 ± 0.003	0.427	
	cg04748988	3	12329223	0.028 ± 0.003	0.033 ± 0.003	**0.001**	*
	cg06573644	3	12329101	0.047 ± 0.012	0.054 ± 0.007	0.207	
	cg07556134	3	12330263	0.011 ± 0.005	0.009 ± 0.007	0.369	
	cg09405169	3	12329745	0.018 ± 0.002	0.020 ± 0.004	0.306	
	cg13518792	3	12329590	0.004 ± 0.003	0.011 ± 0.006	0.169	
	cg18887186	3	12330332	0.067 ± 0.002	0.077 ± 0.007	**0.047**	*
	cg21946299	3	12329166	0.078 ± 0.005	0.079 ± 0.007	0.460	
	cg23514324	3	12329213	0.065 ± 0.035	0.069 ± 0.019	0.386	
	cg26364899	3	12329070	0.042 ± 0.004	0.052 ± 0.009	0.083	
	cg27095527	3	12329080	0.035 ± 0.011	0.038 ± 0.005	0.407	
CEBPD	cg04239843	8	48649767	0.057 ± 0.005	0.059 ± 0.003	0.162	
	cg06734962	8	48650989	0.059 ± 0.006	0.061 ± 0.005	0.273	
	cg13402155	8	48650705	0.050 ± 0.001	0.055 ± 0.005	0.188	
	cg16241714	8	48650511	0.008 ± 0.004	0.005 ± 0.001	0.207	
	cg17194240	8	48651122	0.006 ± 0.002	0.006 ± 0.005	0.486	
	cg18923221	8	48650727	0.063 ± 0.005	0.055 ± 0.004	**0.000**	*
	cg21315018	8	48651635	0.037 ± 0.003	0.041 ± 0.002	0.155	
	cg22280940	8	48650745	0.008 ± 0.002	0.002 ± 0.001	**0.012**	*
	cg23495695	8	48651311	0.010 ± 0.004	0.015 ± 0.002	0.066	
LEP	cg00840332	7	127881269	0.046 ± 0.015	0.044 ± 0.022	0.479	
	cg07464571	7	127881001	0.137 ± 0.045	0.154 ± 0.037	0.183	
	cg12782180	7	127880932	0.154 ± 0.053	0.152 ± 0.042	0.491	
	cg13381984	7	127881344	0.120 ± 0.008	0.145 ± 0.027	0.187	
	cg19594666	7	127881280	0.108 ± 0.030	0.133 ± 0.040	0.318	
	cg26814075	7	127881298	0.186 ± 0.016	0.175 ± 0.012	0.223	

Figure captions

Fig. 1. Macroscopic, radiographic and microscopic observations of the two layers of human subcutaneous tissue. (A) The superficial fascia anatomically separates subcutaneous tissue into superficial adipose tissue (SAT) and deep adipose tissue (DAT). SAT has thick fibrous septa and cuboid-shaped fat lobules, whereas DAT has thin fibrous septa and flat-shaped fat lobules. A magnetic resonance image also shows the structure of the tissue clearly. (B) Hematoxylin-eosin (HE) staining shows the gross anatomical structure of subcutaneous tissue. SAT was confirmed to be thicker than DAT and superficial fascia to be a multi-layered structure. (C) Azan, Masson-Goldner (MG) and Elastica van Gieson (EVG) staining accentuate the superficial fascia consisting of collagenous fibers and nuclei. (D) The number of cells / mm^2 and cell area in each adipose tissue layer, using fatty acid binding protein 4 (FABP4) staining, were compared. n = 3. *P < 0.05.

Fig. 2. Microscopic comparison of the adipogenic status among four populations of primary cultured adipocytes: CS: ceiling culture-derived proliferative adipocytes (ccdPAs) obtained from SAT; CD: ccdPAs obtained from DAT; AS: adipose-derived stem cells (ASCs) obtained from SAT; AD: ASCs obtained from DAT. (A) After incubation with normal medium and confirmation of confluency, the cells were cultured for 14 days in adipogenic differentiation medium. Oil Red O and BODIPY staining was then performed. (B) In BODIPY-stained images

of the four cell types, the stained areas, i.e. areas of droplets per field of view (1.6×10^6 μm^2), were calculated. n = 3. *P < 0.05.

Fig. 3. Evaluation of cellular differentiation in response to partial adipogenic stimulation in the CS and CD cell populations. Three variations of the original medium were used in which one factor each of insulin (INS), 3-isobutyl-1-methylxanthine (IBMX) or dexamethasone (DEX), was removed. Gene expression of the following adipogenic markers was compared by RT-PCR: peroxisome proliferator-activated receptor γ (*PPARG*) (A), CCAAT/enhancer binding protein δ (*CEBPD*) (B) and *LEP* (C). n = 3. *P < 0.05.

Fig. 4. Evaluation of the expression levels of adipogenesis-related genes and proteins in response to adipogenic differentiation stimulation in four populations of cells with or without adipogenic induction (AI): CS, CD, AS, and AD. (A) The mRNA expression levels of *PPARG* were measured and compared by RT-PCR. (B) Western blot bands representing PPAR-γ were seen in each of the differentiated cell populations. The protein expression level was expressed as the band density relative to that of glyceraldehyde-3-phosphate dehydrogenase (GAPDH). (C) The mRNA expression levels for *CEBPD* were measured by RT-PCR. (D) ELISA was performed to evaluate leptin protein secretion. n = 3. *P < 0.05.

Table 1. CpG island methylation of genes related to adipogenesis. Genome-wide methylation

levels of two populations of adipocytes were measured: CS and CD. The beta-values (mean ± SD) of each CpG island within the adipogenesis-related genes *PPARG*, *CEBPD* and *LEP* were compared. Probe ID: the CpG locus ID identified by Illumina. chr: chromosome number from genome reference consortium human build 37 (GRCh37). Map info: the base coordinate from GRCh37. n = 3. *P < 0.05.

American Journal of Physiology – Cell Physiology

平成27年10月13日　投稿中